IV Conferencia Panamericana de END
Buenos Aires – Octubre 2007

Ultrasonic evaluation of closed cracks using subharmonic/ superharmonic phased array and a laser interferometer

K. Yamanaka, Y. Ohara, S. Yamamoto, T. Mihara
Department of Materials Processing, Tohoku University
Aoba 02, Sendai, 980-8579 Japan
Telephone 81-22-795-7357
Telefax 81-22-795-4298
E-mail yamanaka@material.tohoku.ac.jp

Abstract

A new method for detection and sizing of closed crack is described which uses transient waveform of subharmonics with half input frequency in ultrasonic nondestructive evaluation. In analogy to the resonant characteristics of vibration of bubbles in liquids, we formulate an equation for resonant excitation of subharmonics at partially closed cracks. The equation has been partially verified by comparison between experimental and calculated waveforms. An apparatus for imaging closed cracks in critical components such as in atomic power plant **SPACE** (subharmonic phased array for crack evaluation) and its extension using laser interferometer are proposed.

1. Introduction

Although ultrasound is the most sensitive method among nondestructive evaluation methods for detection and sizing of cracks, detection of those without any gap between the crack faces, often referred to as 'closed cracks', is difficult because they are almost transparent to ultrasound. In order to solve this problem, the nonlinear ultrasound of cracks has been extensively investigated [1]-[3], where the superharmonics with integer multiples of input frequency is generated. However, the signal-to-noise (S/N) ratio of superharmonics is not very high, because it is generated in many class of objects such as piezoelectric transducers, liquid coupler and electronic amplifiers. On the other hand, subharmonics with odd multiples of half input frequency has higher S/N because it is generated at more limited object, such as contact between solids [2]-[5] or bubbles in liquid [6]. However, application of subharmonic wave to crack sizing in time domain measurement had not been attempted.

In this situation, we proposed to use subharmonics in closed cracks to reduce error in crack size measurements [7]-[10]. After theoretical [7] and experimental [8] investigation of generation of subharmonic wave at closed cracks, we proposed a nonlinear imaging method and showed a preliminary result on fatigue cracks [9] . We also found a resonant nature of vibration of cracks at a tail part of waveform generated by a large amplitude input wave [10]. Based on those, we propose a framework for crack size measurement using a time domain signal of subharmonic wave.

2. Resonance characteristics of subharmonics

The resonant vibration at subharmonic frequency has been extensively studied for micro bubbles in liquid [6]. It has been verified that the amplitude of a generated subharmonic wave takes a maximum when the input wave frequency is close to twice the vibration resonance frequency of the bubble. On the other hand, a linear resonance occurs when the input wave frequency is close to the resonance frequency, though the resonance frequency is shifted due to the nonlinearity if the input wave amplitude is large.

The resonance-like property of a subharmonic wave of closed cracks can be explained similarly to that of bubbles, as shown in Figure 1. When the input wave amplitude is small, the faces of the closed crack are tightly pressed to each other (dotted curve). Consequently the input wave has no interaction with the crack. However, when the input wave amplitude is larger than a certain threshold, the crack faces are periodically opened (solid curves) and closed (dotted curve) with a clapping contact at the closed position.

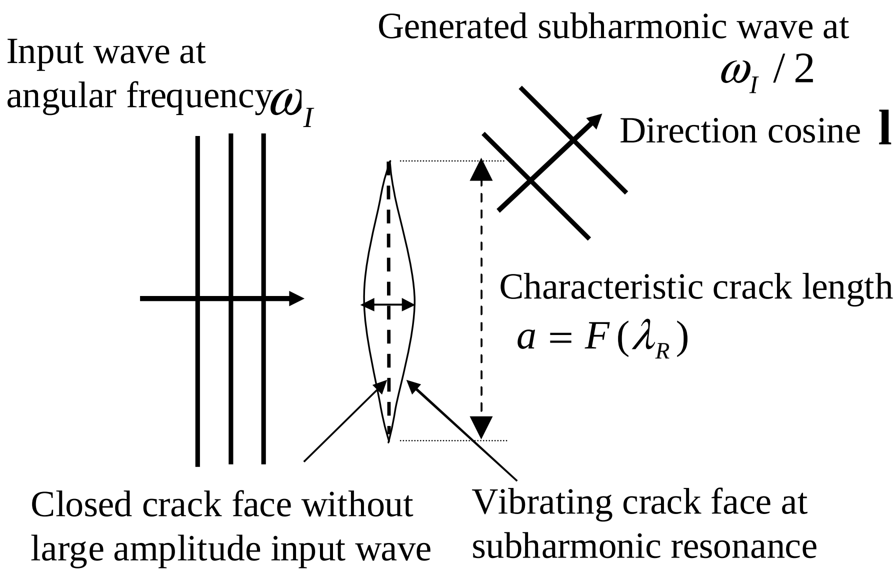

Figure 1. Subharmonic resonance at a closed crack

We define the resonance frequency, ω_R, as an angular frequency of subharmonic wave at $\omega_I / 2$ when it takes the maximum amplitude, as shown in Fig. 2. Here ω_I is the input wave angular frequency. Thus, when ω_I is close to $2\omega_R$, the amplitude u_0 of the generated subharmonic wave takes the maximum as shown in Fig. 2 (a). However, when the subharmonic frequency $\omega_I / 2$ is different from ω_R, the amplitude u_0 is reduced as shown in Fig. 2 (b).

The resonance frequency for a wave generated towards the direction cosine $\mathbf{l}$ from a crack of characteristic length a is formally expressed as

$$\omega_R = F(V, \mathbf{l}, a) \quad (1),$$

where V is the velocity of acoustic wave responsible for the resonance, and $F(V, \mathbf{l}, a)$ is an arbitrary function depending on the shape and physical property of the crack. The characteristic crack length is expressed as

$$a = G(\lambda) \qquad (2),$$

where the functional form of G is determined from function F and λ is the wavelength determined from the velocity V and ω_R.

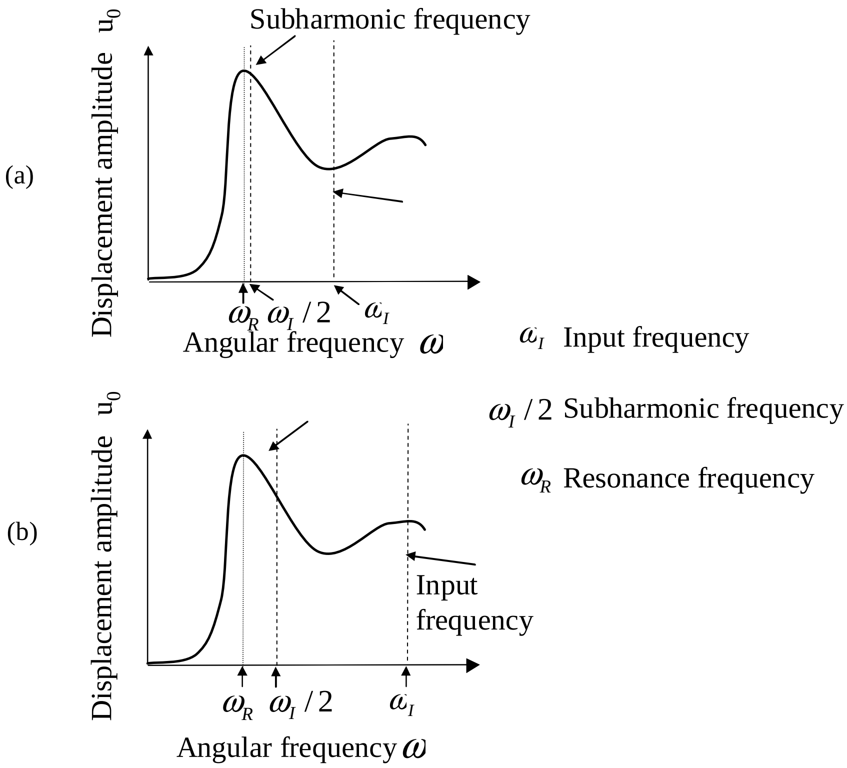

Figure 2. Frequency dependence of subharmonic amplitude

As a special case of a planar elliptical or rectangular crack, the resonance frequency will be close to the peak frequency of scattering cross section in the linear case [12-13],

$$\omega_R = \frac{\pi(2n-1)V_R}{2a} \text{ or } f = \frac{(2n-1)V_R}{4a} \qquad (n = 1,2,3) \qquad (3),$$

where V_R is the Rayleigh wave velocity. For the particular case of eq. (3), eq. (2) becomes,

$$a = (2n-1)\lambda_R / 4 \qquad (n = 1,2,3) \qquad (4).$$

To investigate the nature of nonlinear ultrasound including not only the superharmonics but also subharmonics, we tried to reproduce experimental subharmonic waveform. Although an exact treatment of cracks requires intensive numerical calculations, we employ a simple equation to reproduce an essential feature suitable for obtaining physical insight on the phennomena [7, 10]. In this model, we assume that the output side crack face is driven by the input side crack face whose motion is known and is identical to the displacement waveform of incident waveform.

The approximation gives,

$$\ddot{x} + \Gamma \dot{x} + {\omega_R}^2 (x - x_s) = F^* (x - a \sin \omega_I \ t) \qquad (5)$$

where x is the position of output side crack face, Γ is the normalized damping factor, F^* is the interaction force between two crack faces, and x_s is equilibrium value of x where no interaction force is operated. The force function on the right-hand-side of eq. (1) can be either the extended Lennard-Jones force [7], [10] or a bilinear force. Coefficients of eq. (1) are equivalent to those in [7] and [10], but normalized so that the angular resonance frequency $\omega_R = \sqrt{k/m}$ is used, instead of the stiffness k mass m of the output crack face. Eq. (5) represents a forced vibration excited at an angular frequency, $\omega = \omega_I$. However, if $F^* = 0$, it represents a free vibration at the resonant frequency $\omega = \omega_R$.

3.Time domain measurement of subharmonics

We conducted experiments on a fatigue crack in an aluminum alloy (Al7075). The fatigue crack was extended from a notch in a three-point bending fatigue test up to 15 mm, with a maximum and minimum stress intensity factors of 14 kgf/mm$^{3/2}$ and 2 kgf/mm$^{3/2}$, respectively which were selected to form a closed crack [8]. The subharmonic wave was observed in a transmission configuration using an obliquely incident longitudinal wave with a polystyrene wedge. A sinusoidal wave with a frequency of 7.0 MHz was produced by a wave generator, and this wave of 20 cycles was amplified by a gated amplifier. The displacement amplitude of a longitudinal wave at the crack position was estimated to be larger than 20 nm p-p using a laser interferometer.

The validity of eq. (1) has been partially verified by agreement between experimental and calculated subharmonic waveform [7,10,14] as shown in Fig. 3. The parameters used for the calculation are given in ref. [10]. As the bending force increased the relative magnitude of subharmonics was increased in the experimental results (a), which was reproduced in the calculated results (b). The tail effect showing a single pulse with low center frequency in (a) was also reproduced (b), whose angular frequency is given by the resonance frequency ω_R.

To evaluate the temporal resolution of subharmonic wave and to extract ω_R from experimental waveform, the time-frequency spectrum analysis was performed. Figure 4 (below) shows a subharmonic waveform with tail effect for the same sample as in Fig. 3. Fig. 4 (top) shows a magnitude of wavelet transform using the Gabor function mother wavelet. The input frequency was 7.0 MHz and the subharmonic freqnency was 3.5 MHz. It was shown from the wavelet image that the subharmonic component was established in less than 1 μs. The arrival time (20-21 μs) and frequency (2.5 MHz) of the tail effect was also clearly observed in the wavelet image. Since the frequency of tail effect is approximately equal to the resonance frequency according to eq. (1), the resonance frequency is estimated to be 2.5 MHz.

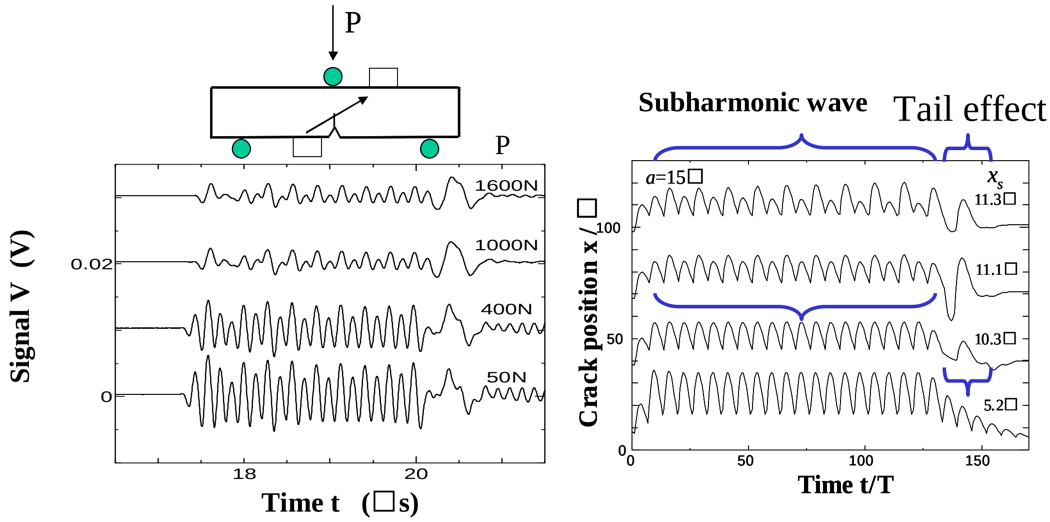

(a) Experimental results (b) Calculated result

Figure 3. Subharmonic waveforms

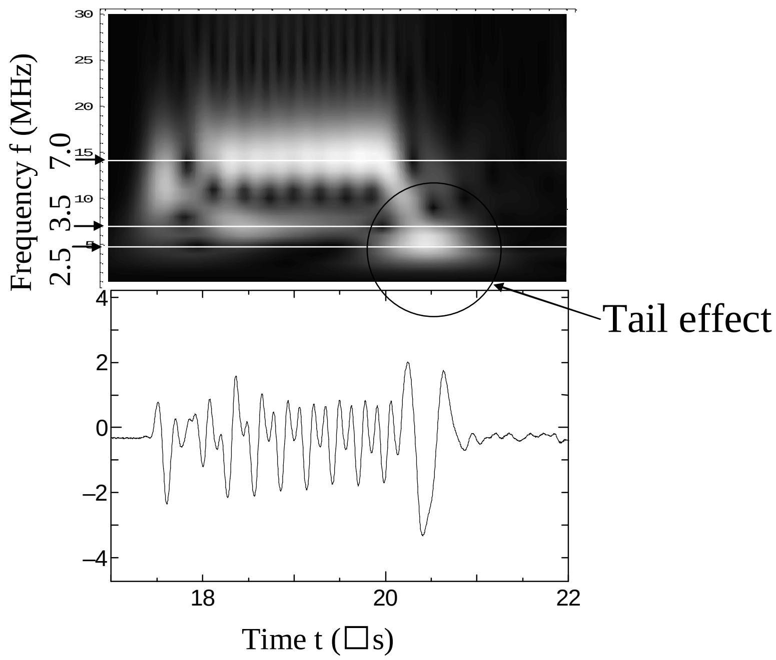

Figure. 4. Wavelet transform of subharmonic wave and tail effect in transmission configuration

In a reflection configuration advantageous for crack size measurement, we developed a nonlinear imaging method SPACE (subharmonic phased array for crack evaluation). [9,16]. We show a preliminary result for subharmonic imaging of the same specimen.

To irradiate cracks with the intense ultrasound required to generate subharmonic waves, we fabricated a LiNbO3 single-crystal transmitter. As an input signal for the transmitter, we used a three-cycle tone burst of a 7 MHz sinusoidal wave. Although the particle displacement amplitude at a crack in an aluminum specimen can be larger than 20 nm, we set it at 10 nm, slightly above the subharmonic generation threshold. This is because there is a broad optimum range of input power for observing clear subharmonic resonance, as reported for bubbles in medical ultrasonic diagnosis21. As a receiver, an array sensor with a center frequency of 5 MHz was used for both fundamental and subharmonic components. To produce images, propagation times along the paths such as A-B-C-D in Fig. 5 were calculated and subtracted before the summation of signals received from each element of the array sensor. To filter the received signals at fundamental and subharmonic frequencies, digital band-pass filters were applied. Thus, the apparatus is able to selectively image closed and open cracks.

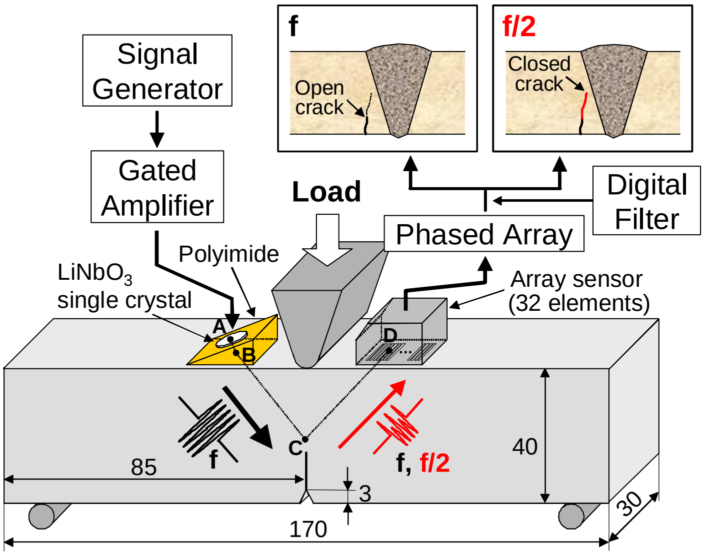

Figure 5. Subharmonic imaging apparatus SPACE

To verify the performance of the apparatus, we formed well-defined closed cracks in aluminum alloy (Al7075) specimens using a three-point bending fatigue test. Figure 6 shows the fundamental and subharmonic images of cracks in the aluminum alloy specimens. In the high-stress-intensity sample, the crack tip was clearly observed in the fundamental image [Fig. 6(a)], whereas it was invisible in the subharmonic image [Fig. 6(b)]. This result shows that the crack tip was open. It was also confirmed that the location of the crack tip in the obtained image agreed with that of the actual crack tip on the side wall shown in the photograph [Fig. 6(c)]. In contrast, in the low-stress-intensity sample, the crack tip was invisible in the fundamental image [Fig. 6(d)], whereas it was clearly observed in the subharmonic image [Fig. 6(e)]. This result shows that the crack tip was partially closed. Thus, we demonstrated that the subharmonic image indicates the accurate location of closed cracks [16].

Though a resonance is advantageous for increasing the magnitude of response, the input frequency does not have to be precisely tuned to the resonance frequency because the sharpness of the resonance is not large in general. Consequently, cracks of varied length can be evaluated by a single input frequency. Nevertheless, variable frequency transmitter is highly desired to cover wide range of crack length.

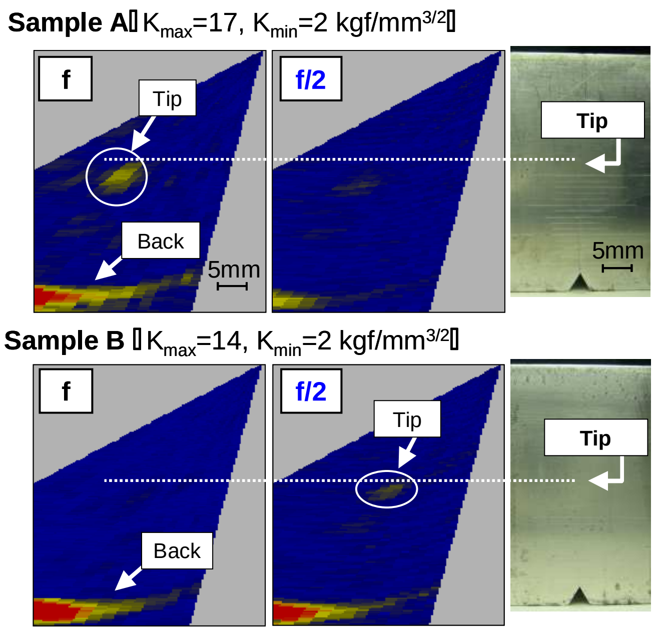

Figure 6. Image of SPACE

To study the nonlinear process more quantitatively, it is desirable to measure displacement at many points on the surface. As an approach for this goal, we proposed a laser SPACE where detection is made by scanning laser interferometer as shown in Fig. 7. The detailed description will be given elsewhere.

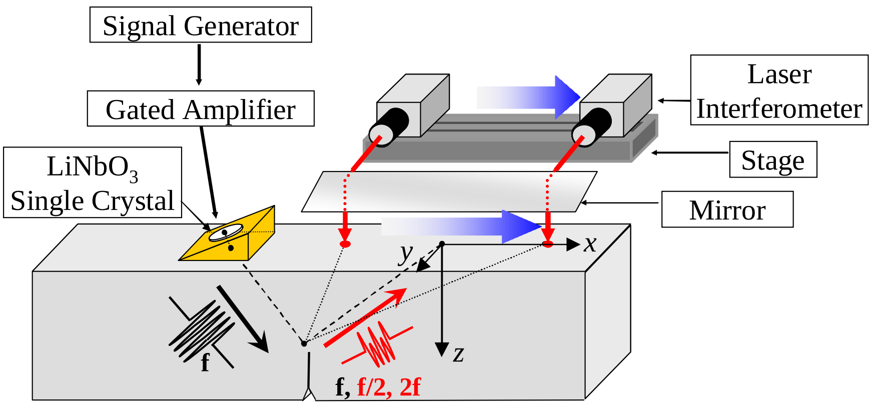

Figure 7. Laser SPACE

In a theoretical aspect, eq. (1) is valid in the limit of large crack face penetrating the object, when the input and output sides are clearly defined [14]. For smaller cracks not penetrating the object, it is still effective as a first approximation to reproduce many aspects of subharmonic wave [7,10,14,15]. However, further improvement is required for more quantitative comparison with experiment. The next approach is made by introducing a one dimensional elastic body in the model and by discriminating the transmission and reflection configurations.

4. Conclusion

We proposed a framework for crack size measurement using a time domain signal of subharmonic wave. In analogy to the resonant characteristics of subharmonic vibration of bubbles in liquids, we formulate resonant excitation of subharmonic wave from partially closed cracks. The presence of resonance has been partially verified by resembrance between experimental waveform and calculated waveform by a single-degree-of freedom equation of resonant vibration.

Acknowledgement

This work was supported by the fellowship of Japan Society for the Promotion of Science for Young Scientists, and by Grant in Aid for Science Research (No. 16206071) from the Ministry of Education, Culture, Sports, Science and Technology.

References and footnotes

[1] O. Buck, W.L. Morris and J.M. Richardson: Appl. Phys. Lett. 33 (1978) 271.
[2] B.A. Korshak, I.Yu. Solodov and E.M. Ballad: Ultrasonics 40 (2002) 707.
[3] A. Moussatov, V. Gusev and B. Castagnede: Phys. Rev. Lett. 90 (2003) 124301.
[4] I. Y. Solodov, N. Krohn and G. Busse: Ultrasonics 40 (2002) 621.
[5] E. M. Abdel-Rahman and A. H. Nayfeh, Nanotechnology 16 (2005) 199.
[6] P.M. Shanker, P.D. Krishna and V.L. Newhouse: J. Acoust. Soc. Am. 106 (1999) 2104.
[7] K. Yamanaka, T. Mihara and T. Tsuji: Jpn. J. Appl. Phys. 43 (2004) 3082.
[8] M. Akino, T. Mihara and K. Yamanaka: Review of Progress in Quantitative Nondestructive Evaluation 23 (2004) 1256.
[9] Y. Ohara, T. Mihara and K. Yamanaka : The third US-Jpn. Symp. on Nondestructive Evaluation (2005) 229.
[10] R. Sasaki, T. Ogata, Y. Ohara, T. Mihara and K. Yamanaka, Jpn. J. Appl. Phys. 44 (2005) 4389.
[11] J.D. Achenbach, L.M. Keer, & D.A. Mendelsohn, J. Appl. Mech. 47 (1980) 551.
[12] D. E. Budreck and J. D. Achenbach, J. Appl. Mech. 55 (1998) 405.
[13] L. Guan and A. Norris, Int. J. Solids Structures 29 (1992) 1549.
[14] K. Yamanaka, R. Sasaki, T. Ogatga, Y. Ohara and T. Mihara, Rev. Prog. QNDE 25 (2006) 283.
[15] Y. Ohara, T. Mihara, and K. Yamanaka, Ultrasonics, 44, 194-199 (2006).
[16] Y. Ohara, T. Mihara, R. Sasaki, T. Ogata, S. Yamamoto, Y. Kishimoto, and K. Yamanaka, Appl. Phys. Lett., 90, 011902-1-3 (2007).